LAWRENCE
LIVERMORE
NATIONAL
LABORATORY

LLNL-CONF-423083

Event-by-Event Study of Prompt Neutrons from 239Pu

R. Vogt, J. Randrup, J. Pruet, W. Younes

February 2, 2010

NEDPC 2009
Livermore, CA, United States
October 26, 2009 through October 30, 2009

Disclaimer

Event-by-Event Study of Prompt Neutrons from ^{239}Pu (U)

R. Vogt[1], J. Randrup[2], J. Pruet[1] and W. Younes[1]

.[1]LLNL, Livermore, CA, USA

[2]LBNL, Berkeley, CA, USA

Employing a recently developed Monte Carlo model, we study the fission of ^{240}Pu induced by neutrons with energies from thermal to just below the threshold for second chance fission. Current measurements of the mean number of prompt neutrons emitted in fission, together with less accurate measurements of the neutron energy spectra, place remarkably fine constraints on predictions of microscopic calculations. In particular, the total excitation energy of the nascent fragments must be specified to within 1 MeV to avoid disagreement with measurements of the mean neutron multiplicity. The combination of the Monte Carlo fission model with a statistical likelihood analysis also presents a powerful tool for the evaluation of fission neutron data. Of particular importance is the fission spectrum, which plays a key role in determining reactor criticality. We show that our approach can be used to develop an estimate of the fission spectrum with uncertainties several times smaller than current experimental uncertainties for outgoing neutron energies of less than 2 MeV. (Classification)

Introduction

Despite the many theoretical advances, there is not yet a quantitative theory of fission. This is unfortunate because nuclear fission remains important to society at large due to its many practical applications, including energy production and security. For example, reactors and other critical systems demand that neutron growth be known to about the 0.1% level for model simulations to be reliable. In such cases, scattering experiments are insufficiently accurate, requiring reliance on more inclusive, higher statistics integral critical assembly experiments.

Furthermore, in the last few years, efforts have been made to develop systems capable of detecting concealed nuclear material. These applications place entirely different demands on fission models by attempting to exploit specific information carried by particles resulting from fission. Thus there is a need for a fission description that accounts for particle correlations and fluctuations on an event-by-event level. Such a description, employing a model incorporating the relevant physics with a few key parameters, compared to the pertinent data through a statistical analysis, presents a potentially powerful tool for bridging the gap between current microscopic models and important fission observables and for improving estimates of the relatively gross fission characteristics important for applications. This type of approach also provides a means of using readily measured observables to constrain our understanding of the microscopic details of fission.

Relatively recently, Lemaire *et al.*[1] implemented a Monte Carlo simulation of statistical decays of fission fragments by sequential neutron emission for spontaneous fission of ^{252}Cf and thermal fission of ^{235}U. That work demonstrated how such simulations, in conjunction with experimental data and models of the relevant physics, can be used to predict the neutron spectrum and to validate and improve the underlying physics models.

In the present work, we have implemented a similar Monte Carlo-based approach and applied it to calculate sequential neutron emission from the ^{240}Pu compound nucleus created from the reaction n+^{239}Pu. The ^{239}Pu fission cross section changes significantly for $0.5 \leq E_n \leq 5.5$ MeV, making applications very sensitive to incident neutrons in the few MeV region.

We have adapted the recently developed fission event generation FREYA[2] to calculate the production and decay of fission fragments and used maximum-likelihood analysis to estimate properties of the emitted fission neutrons and their correlation coefficients. The detailed statistical analysis presented here is essential for developing a more quantitative understanding of fission and thus obtaining better evaluations of fission data for various applications.

FREYA follows each fission event from the birth of the excited fragments through their decay via prompt neutron emission until the fragment excitation energy is below the neutron separation energy. It also includes the subsequent gamma emission from each fragment, albeit in a rather preliminary way.

We assume binary fission of the compound nucleus, e.g. ^{240}Pu, with mass A_c and charge Z_c formed by incident neutrons of energy E_n on an actinide with mass A_c - 1, e.g. ^{239}Pu. The identities of the hot, excited fission fragments are obtained by sampling the mass and charge of the light, L, and heavy, H, fragments from fission fragment distributions, ensuring mass and charge. The fission Q value is determined from the mass and charge of the fission fragments and subsequently divided into the total fragment kinetic and excitation energies. We make an initial estimate of the total fragment kinetic energy, TKE, by sampling the kinetic energy due to mutual Coulomb repulsion,
TKE = $Z_L Z_H e^2/(R_L + R_H + s(E_n)\, d_{LH}(A_H, E_{\mathrm{thermal}}))$.
Here Z_i and R_i are the charges and radii of the fragments, d_{LH} is the tip separation distance between the fragments at scission, extracted from measurements of the TKE as a function of the heavy fragment mass, A_H, obtained from experiments with thermal neutrons, E_{thermal}, and $s(E_n)$ is an energy-dependent scale factor. The total fragment excitation energy is found using energy conservation, TEE = Q – TKE. This TEE is divided between the light and heavy fragments and translated into a fragment temperature assuming $E_i^* = a_i\, T_{LH}^2$ where $a_i = A_i/e_0$ and e_0 is an asymptotic level density parameter. Allowing for temperature fluctuations in small systems, we modify the excitation energies by their thermal fluctuations. We adjust the TKE accordingly to retain total energy conservation.
Neutrons are then evaporated from the excited fragments until the excitation energy is too low for further neutron emission. Prompt gamma emission follows after prompt neutron emission ceases. So far, the fission neutron spectrum has been evaluated up to the threshold for neutron emission before fission. Multi-chance fission for values of E_n greater than a few MeV has yet to be implemented.

There are significant uncertainties in our overall understanding of fission. To reduce these uncertainties, we need to look at the ‘big picture’, not just spectra since other physics processes feed into these spectra. Both the average neutron multiplicity, $<\nu>$, and the spectra, $d<\nu>/dE$, depend on the physics of the fission process. The multiplicity and the spectra are intimately linked and can’t really be treated separately in a realistic fission model. Thus improvements in the spectral evaluation will come with improved modeling of fission.

Spectral data for thermal neutrons are inconsistent with each other and have large uncertainties in important regions, see Fig. 1, much larger than the constraints on $<\nu>$ itself. The published spectral data do not extend into the low energy region of less than 100 keV. These data are also not generally available for incident neutrons of more than a few MeV, see Fig. 2, making extrapolation necessary. Measurements of other quantities that could guide model calculations, such as total fragment kinetic energy and neutron multiplicity as a function of fragment mass, only exist for thermal incident energies, E_{thermal}. Modeling complete fission events with FREYA helps fill the gaps in data.

To obtain the best possible agreement between the neutron multiplicity and the neutron spectra, three FREYA parameters have been ‘tuned’ in two possible scenarios[3]: either to both the spectral data and $<\nu>$ or to the more accurate measurements of $<\nu>$ alone.

1. The factor $s(E_n)$ which scales the average fragment tip separation distance, d_{LH}, obtained from the experimental TKE(A_H);
2. The asymptotic level density parameter, e_0, which sets the fragment ‘temperature’ for neutron evaporation;

3. The relative excitation of the light and heavy fragments, x, with $E_L^* = x a_L \mathrm{TEE}/(a_L+a_H)$, $E_H^* = \mathrm{TEE} - E_L^*$. Here $x = 1$ is the equal temperature situation, resulting in same number of neutrons emitted from both fragments; $x > 1$ means more neutrons are evaporated from the light fragment than the heavy fragment.

Results

Figures 1 and 2 show the spectral data we have used in our comparison. The uncertainties are not given for all the data shown. In these cases we have assigned a 5% uncertainty to the data, comparable to the typical uncertainties associated with other spectra data. Note that in Fig. 1, the discrepancies between the data sets for $E < 1$ MeV can be rather large. These data were taken at $E_n < 0.5$ MeV and are not absolutely normalized. To compare the data sets and our results most straightforwardly, we normalize all data sets, as well as our calculations, to unity using a Watt spectrum.

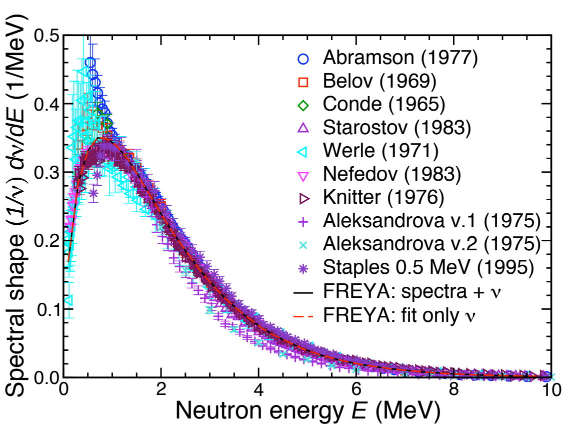

Fig. 1. The measured prompt neutron energy spectra[4,5,6,7,8,9,10,11,12], normalized to unity, as a function of outgoing neutron energy for E_n<*0.5* MeV[3].

Figure 2 shows data taken over a range of incident neutron energies, $0.5 \le E_n \le 3.5$ MeV. In this case, the data and the calculations are not normalized to unity but to $<\nu>$ since the multiplicity increases with energy to be able to distinguish between the curves.

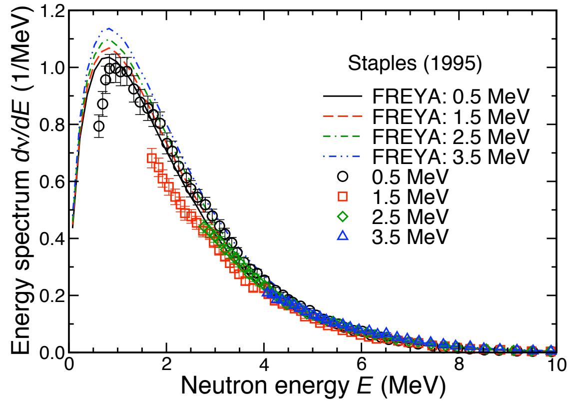

Fig. 2. The measured prompt neutron energy spectra[12] as a function of outgoing neutron energy for E_n = *0.5, 1.5, 2.5* and *3.5* MeV[3].

Two measurements that provide more detailed information with which to tune models to the underlying physics of fission are shown in Figs. 3 and 4, the total kinetic energy as a function of heavy fragment mass, TKE(A_H), and the neutron multiplicity, ν, as function of fragment mass, respectively. Both are shown for thermal neutrons incident on ^{239}Pu and compared to `FREYA` calculations.

There are no uncertainties shown on the TKE in Fig. 3. The vertical bars indicate the full-width at half-maximum of the TKE distribution at several values of A_H. Near symmetric fission, the fission fragments are mid-shell nuclei subject to strong deformation, resulting in a large tip separation distance and a low TKE. At $A_H = 132$, the heavy fragment is close to a doubly-magic closed shell ($Z_H = 50$, $N_H = 82$) and is resistant to distortions, remaining more spherical, while the light fragment is significantly deformed. This combination results in a smaller tip separation and thus a larger TKE. The model calculations reproduce this behavior rather well.

The multiplicity of the neutrons emitted by the hot fragments as they de-excite has a characteristic sawtooth shape for incident thermal neutrons. This follows from the TKE observed in Fig. 3. The peak in $\nu(A)$ near symmetry is due to the larger excitation energy corresponding to the lower TKE. The drop in $\nu(A)$ around $A = 130$ can be attributed to the lower excitation energy of the closed shell nucleus. The sawtooth character of the multiplicity distribution is likely to be reduced as the incident energy increases since the excitation energy increases the overall multiplicity and binary fission produces more mass-symmetric fragments. Unfortunately, no data are available at higher than thermal energies to study the energy dependence of these observables in detail.

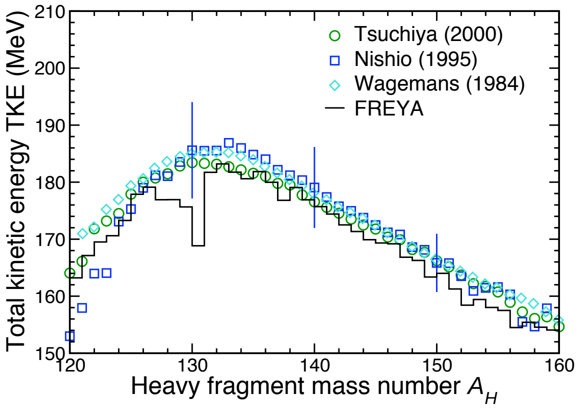

Fig. 3. The measured average TKE[13,14,15] as a function of heavy fragment mass number, compared to FREYA results[3].

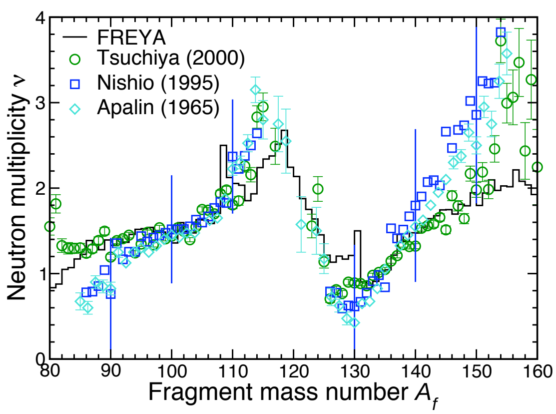

Fig. 4. The average neutron multiplicity[13,14,16] as a function of fragment mass number, compared to FREYA results[3].

Covariances

In addition to single particle observables, it is interesting to consider correlations in the spectral strengths at different energies. The diagonal elements of the covariance matrix are the squares of the standard deviations in the model calculations. The off-diagonal matrix elements give the covariances between two outgoing energies. The covariance matrix between spectral strengths at different outgoing neutron energies is defined as $\sigma(E_k,E_{k'}) = \langle(E_k - \langle E_k\rangle)(E_{k'} - \langle E_{k'}\rangle)\rangle$.
For continuous observables, such as spectra, there is a singularity along the diagonal,
$\sigma(E_k,E_{k'}) = \langle\sigma_k^2\rangle\delta(E_k-E_{k'}) + \langle\sigma_{k,k'}\rangle$
where $\langle\sigma_k^2\rangle$ is the variance in the differential yield at E_k while $\langle\sigma_{k,k'}\rangle$ is the correlation between yields at two different energies, E_k and $E_{k'}$. After the singular part has been removed, the correlation coefficient matrix is $C(E_k,E_{k'}) = \langle\sigma_{k,k'}\rangle/(\langle\sigma_k\rangle\langle\sigma_{k'}\rangle)$.
The result for $E_n = 0.5$ MeV when fitting to $\langle\nu\rangle$ alone is shown in Fig. 5. The cross-diagonal lines are lines of constant total energy, $E_T = E_k + E_{k'}$. The values of the correlation matrix along these lines are shown in Fig. 6.

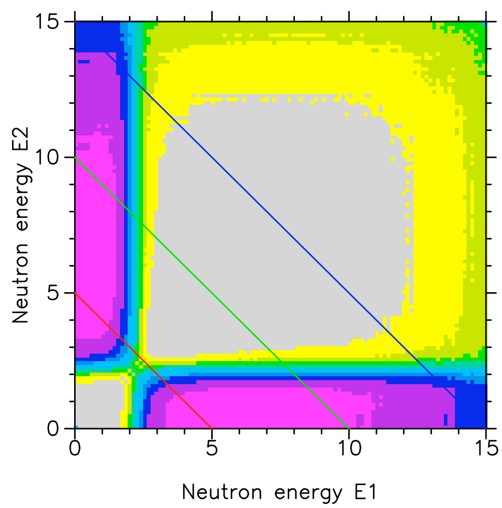

Fig. 5. The correlation coefficients, *C(Ek,Ek')*, for the spectral strength of neutrons evaporated from the excited fragments. Cuts along lines of constant total energy of E_T = *5, 10,* and *15* MeV are shown[3].

When the model parameters are varied, the spectral shapes tend to pivot around $E \approx 2$ MeV. Thus, when both neutron energies lie on the same side of this value, the differential changes are in phase and the correlation coefficient is close to unity. The changes are in opposite directions when the two energy values are on opposite sides of the pivot energy and $C(E_k,E_{k'})$ is close to *-1*. The results for constant E_T in Fig. 6 show this behavior more clearly.

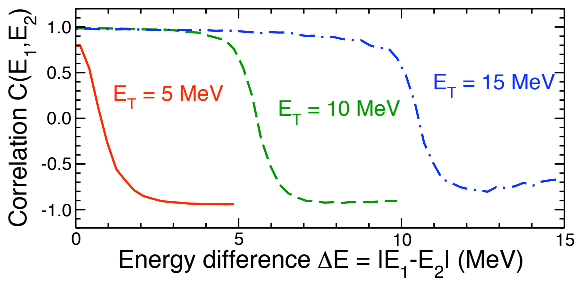

Fig. 6. The spectral correlation coefficients $C(E_1,E_2)$, along the three lines of constant total energy indicated in Fig. 5 as a function of the energy difference, $\Delta E = |E_1 - E_2|$[3].

Comparison to Existing Work

Here we compare our preliminary `FREYA` results with the present `ENDF/B-VII` evaluation[17] (Fig. 7) and with some plutonium critical assemblies (Fig. 8).

Our spectra are systematically softer, giving lower mean neutron energies. This difference has implications for criticality.

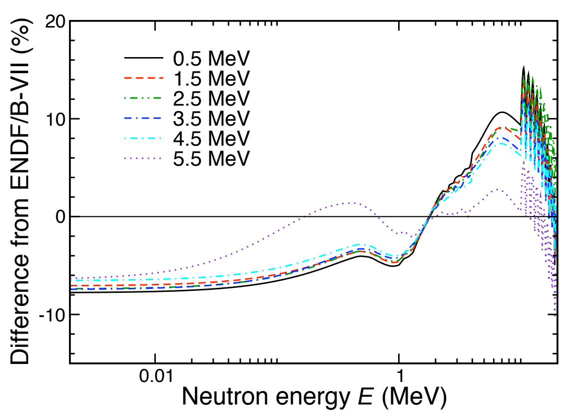

Fig. 7. The percentage difference between our evaluated spectra and that of `ENDF/B-VII` for all six incident neutron energies considered[3].

While the softer spectrum decreases the calculated values of k_{eff} by about *0.003*, there is relatively good agreement with the measured k_{eff} in Fig. 7. Because there is an approximate 1.5 standard deviations difference relative to the JEZEBEL result, this may indicate that the Pu fission cross section or the neutron multiplicity may be low by about 0.1%.

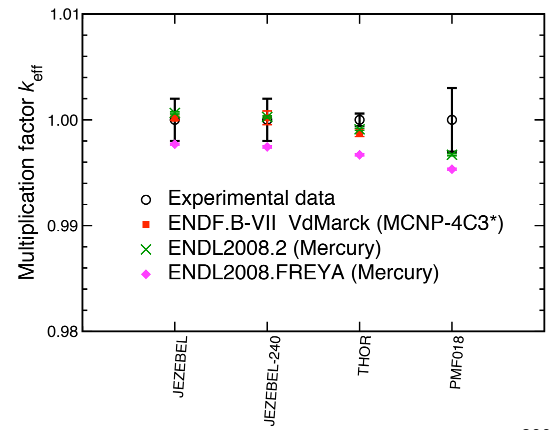

Fig. 7. The calculated k_{eff} for several ^{239}Pu critical assemblies using our spectra (diamonds) in the `Mercury` Monte Carlo for $0.5 \le E_n \le 5.5$ MeV[3]. The results are compared to those employing the standard `ENDF/B-VII`[17] (squares) and `ENDL2008.2`[18] (crosses) databases.

Summary

We have shown that the evaluated neutron spectra not are strongly influenced by the spectral data, $<\nu>$, with its much smaller associated uncertainty is more important. Improvements in modeling will come from better knowledge of the complicated fission process through microscopic models and high statistics, less inclusive data.

`FREYA` bridges models and data by addressing complete events with full energy-momentum conservation and correlations between observables. The next step is to include multi-chance fission in `FREYA` to address higher incident neutron energies.

Acknowledgments

This work was performed under the auspices of the U.S. Department of Energy by Lawrence Livermore National Laboratory under Contract DE-AC52-07NA27344 (RV, JP, WY), by Lawrence Berkeley National Laboratory under Contract DE-AC02-05CH11231 (JR) and was also supported in part by the National Science Foundation Grant NSF PHY-0555660 (RV).

References

1. Lemaire S, Talou P, Kawano T, Chadwick M B, and Madland D G, "Monte Carlo approach to sequential neutron emission from fission fragments", Phys. Rev. C **72**, 024601 (2005).

2. Randrup J and Vogt R, "Calculation of fission observables through event-by-event simulation", Phys. Rev. C **80,** 024601 (2009).

3. Vogt R, Randrup J, Pruet J, and Younes W, "Event-by-event study of prompt neutrons from ^{239}Pu(n,f)", Phys. Rev. C **80**, 044611 (2009).

4. Abramson D and Lavelaine C, "Fission neutron spectra of ^{235}U and ^{239}Pu", A.E.R.E. Harwell Report 8636 (1977), http://www-nds.iaea.org/exfor/servlet/X4sGetSubent?subID=20997004.

5. Belov L M, Blinov M V, Kazarinov N M, Krivokhatskjj A S, and Protopopov A N, "Spectra of fission neutrons of ^{244}Cm, ^{242}Pu and ^{239}Pu", Yad. Fiz. **9**, 727 (1969), http://www-nds.iaea.org/exfor/servlet/X4sGetSubent?subID=40137004.

6. Conde H and During G, "Fission neutron spectra, part II, fission neutron spectra of ^{235}U, ^{239}Pu and ^{252}Cf", Ark. Fys. **29**, 313 (1965), http://www-nds.iaea.org/exfor/servlet/X4sGetSubent?subID=20575006.

7. Starostov B I, Nefedov V N, and Bojcov A A, "High precision prompt neutron spectra measurement for neutrons from ^{252}Cf, ^{233}U, ^{235}U and ^{239}Pu fission in the energy range 2-11 MeV", *6th All-Union Conf. on Neutron Phys.,* Kiev, Ukraine **2**, 290 (1983), http://www-nds.iaea.org/exfor/servlet/X4sGetSubent?subID=40872003.

8. Werle H and Bluhm H, "Fission neutron spectra measurements of ^{235}U, ^{239}Pu and ^{252}Cf", J. Nucl. Energy **26**, 165 (1972), http://www-nds.iaea.org/exfor/servlet/X4sGetSubent?subID=20616005.

9. Nefedov V N, Starostov B I, and Bojcov A A, "High precision spectra measurements for neutrons arising from the fission of ^{252}Cf, ^{233}U, ^{235}U and ^{239}Pu in the energy range 0.04-5 MeV", *6th All-Union Conf. on Neutron Phys.,* Kiev, Ukraine **2**, 285 (1983), http://www-nds.iaea.org/exfor/servlet/X4sGetSubent?subID=40871006.

10. Knitter H, "Measurement of the energy spectrum of prompt neutrons from the fission of ^{239}Pu by 0.215 MeV neutrons", Atomkernenerg. **26**, 76 (1975), http://www-nds.iaea.org/exfor/servlet/X4sGetSubent?subID=20576003.

11. Aleksandrova Z A, Bol Shov V I, Kuznetsov V F, Smirenkin G N, and Tarasko M Z, "Spectra of secondary neutrons at fission of ^{235}U and ^{239}Pu by neutrons with 0.1 MeV energy", At. Energ. **38**, 108 (1975), http://www-nds.iaea.org/exfor/servlet/X4sGetSubent?subID=40358002; http://www-nds.iaea.org/exfor/servlet/X4sGetSubent?subID=40358003.

12. Staples P, Egan J J, Kegel G H R, Mittler A, and Woodring M L, "Prompt fission neutron energy spectra induced by fast neutrons", Nucl. Phys. A **591**, 41 (1995), http://www-nds.iaea.org/exfor/servlet/X4sGetSubent?subID=13982003.

13. Tsuchiya C, Nakagome Y, Yamana H, Moriyama H, Nishio K, Kanno I, Shin K, and Kimura I, "Simultaneous measurement of prompt neutrons and fission fragments for ^{239}Pu(n_{th},f)", J. Nucl. Sci. Technol. **37**, 941 (2000), http://www-nds.iaea.org/exfor/servlet/X4sGetSubent?subID=22650003; http://www-nds.iaea.org/exfor/servlet/X4sGetSubent?subID=2260005.

14. Nishio K, Nakagome Y, Kanno I, and Kimura I, "Measurement of fragment mass dependent kinetic energy and neutron multiplicity for thermal neutron induced fission of ^{239}Pu", J. Nucl. Sci. Technol. **32**, 404 (1995), http://www-nds.iaea.org/exfor/servlet/X4sGetSubent?subID=23012006; http://www-nds.iaea.org/exfor/servlet/X4sGetSubent?subID=23012005.

15. Wagemans C, Allaert E, Deruytter A, Barthelemy R, and Schillebeeckx P, "Comparison of the energy and mass characteristics of the ^{239}Pu(n_{th},f) and the ^{240}Pu(sf) fragments", Phys. Rev. C **30**, 218

(1984), http://www-nds.iaea.org/exfor/servlet/X4sGetSubent?subID=21995038.

16. Apalin V F, Gritsyuk Yu N, Kutikov I E, Lebedev V I, and Mikaelian L A, "Neutron emission from ^{233}U, ^{235}U and ^{239}Pu fission fragments", Nucl. Phys. A **71**, 553 (1965), http://www-nds.iaea.org/exfor/servlet/X4sGetSubent?subID=41397002.

17. Chadwick M B, *et al*., "`ENDF/B-VII.0`: Next generation evaluated nuclear data library for nuclear science and technology", Nucl. Data Sheets **107**, 2931 (2006).

18. Brown D A, *et al*., "Release of the 2008 Evaluated Nuclear Data Library (`ENDL2008`)", LLNL-TR-413190 (2009).